Steerable miniature jumping robot

**Mirko Kovač · Manuel Schlegel ·
Jean-Christophe Zufferey · Dario Floreano**

Abstract Jumping is used in nature by many small animals to locomote in cluttered environments or in rough terrain. It offers small systems the benefit of overcoming relatively large obstacles at a low energetic cost. In order to be able to perform repetitive jumps in a given direction, it is important to be able to upright after landing, steer and jump again. In this article, we review and evaluate the uprighting and steering principles of existing jumping robots and present a novel spherical robot with a mass of 14 g and a size of 18 cm that can jump up to 62 cm at a take-off angle of 75°, recover passively after landing, orient itself, and jump again. We describe its design details and fabrication methods, characterize its jumping performance, and demonstrate the remote controlled prototype repetitively moving over an obstacle course where it has to climb stairs and go through a window. (See videos 1–4 in the electronic supplementary material.)

Keywords Jumping robots · Bioinspired locomotion · mobile robot · Space robotics

M. Kovač (✉) · M. Schlegel · J.-C. Zufferey · D. Floreano
Laboratory of Intelligent Systems, Ecole Polytechnique Fédérale de Lausanne, 1015 Lausanne, Switzerland
e-mail: mirko.kovac@epfl.ch

M. Schlegel
e-mail: manuel.schlegel@epfl.ch

J.-C. Zufferey
e-mail: jean-christophe.zufferey@epfl.ch

D. Floreano
e-mail: dario.floreano@epfl.ch

1 Introduction

Locomotion in rough terrain is more difficult if the system is small in size. This effect is usually referred to as the "Size Grain Hypothesis" (Kaspari and Weiser 1999), which is described as an "increase in environmental rugosity with decreasing body size". In nature, many small animals, such as locusts (Bennet-Clark 1975), springtails (Bracken-bury and Hunt 1993), click beatles (Alexander 2003) and fleas (Gronenberg 1996) solve this problem by using jumping as their main means of locomotion, as it allows them to overcome relatively large obstacles despite their small body size. An advantage for small systems is however, that the impact forces on landing scale with their mass and therefore it is much less harmful for small and light weight systems to fall compared to big and heavy systems (Alexander 1988). The locomotion strategy of many small animals is thus to jump, upright themselves after landing, reorient and jump again. Different mechanisms and behaviors have been described that allow them to do this (Faisal 2001; Frantsevich 2004).

In robotics, several small jumping robots have been presented so far (Scarfogliero et al. 2007; Lambrecht et al. 2005; Sugiyama et al. 2005; Kovac et al. 2008) but theses systems are not able to upright and steer. In this article we focus on uprighting and steering for jumping robots and we present a novel spherical system with a mass of only 14 g (Fig. 1) that is able to jump, upright itself after landing, steer and jump again.

To date, other jumping robots that are able to upright after landing and steer have been presented (Fig. 2), but they are relatively heavy with a mass between 0.2 kg and 2.5 kg. This leads to relatively high impact forces on landing and limits their applicability in situations such as space exploration where small size and minimal weight are of very high importance (Yim et al. 2003).

Fig. 1 Prototype with a mass of 14 g. The cage has a height of 18 cm and allows the robot to upright itself after landing, steer and jump again

The "Sandia hopper" (A) (Weiss 2001) is a 2.5 kg system that jumps by using a piston driven combustion chamber mounted inside a spherical, plastic shell. After landing it remains in its stable position and can rotate its center of mass in order to change its orientation and jump again. The stair hopping "scout robot" (B) (Stoeter et al. 2002) is a wheeled system of 200 g that jumps using a spring that is coiled around its body. Locomotion in a given direction is ensured by turning the robot prior to jumping. The "minimalist jumping robot" (C) (Burdick and Fiorini 2003) has a mass of 1.3 kg and can, after landing, extend its structure actively and upright for the next jump. The change of direction happens by rotating on its foot. The *Jollbot* (D) (Armour et al. 2007) is a 465 g robot that can actively squeeze its spherical structure in order to upright after landing and can change the direction of its jump by rotating its center of gravity around its main axis. The "rescue robot" (E) (Tsukagoshi et al. 2005) has a mass of 2 kg and can, due to its semispheres on the sides of the wheels, upright on landing, then turn using its wheels very similar to the "scout robot" (B) and jump using a pneumatic drive. Table 1 sum-
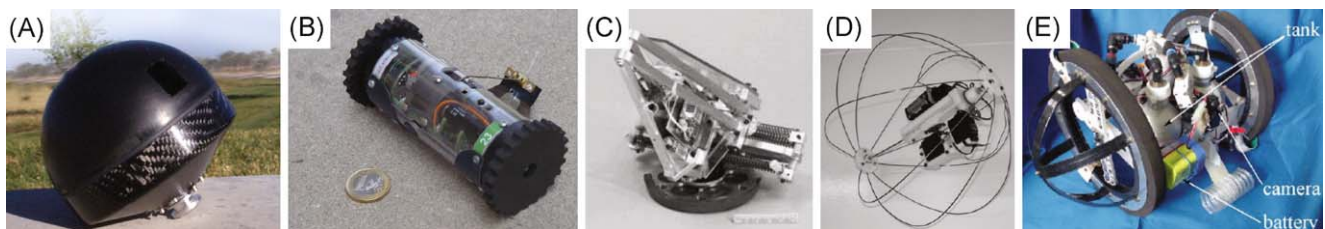
Fig. 2 Overview of existing jumping robots that are able to perform repetitive steered jumps. (**A**) "Sandia hopper" (Weiss 2001) (picture is courtesy of Sandia National Laboratories), (**B**) "stair-Hopping scout robot" (Stoeter et al. 2002) (reprinted by permission of IEEE), (**C**) "minimalist Jumping Robot", v2 (Burdick and Fiorini 2003) (reprinted by permission of SAGE), (**D**) *Jollbot* (Armour et al. 2007) (reprinted by permission of IOP), (**E**) "rescue robot" (Tsukagoshi et al. 2005) (reprinted by permission of IEEE)

Table 1 Steerable jumping robot comparison

Name (Fig. 2)	Mass [g]	Max. size [cm]	Jump height [cm]	Jump distance [cm]	Jump height per mass [cm/g]	Jump height per size [–]	Uprighting principle (Fig. 4)	Steering principle (Fig. 5)
(A) Sandia robot (Weiss 2001)	2500	20	300	300	0.12	15	(C)	(B)
(B) Stair-Hopping scout robot (Stoeter et al. 2002)	200	11	30	20	0.15	2.7	(C)	(A)
(C) Minimalist jumping robot (Burdick and Fiorini 2003)	1300	15	90	200	0.07	6	(A)	(C)
(D) Jollbot (Armour et al. 2007)	465	30	21.8	0	0.06	1.4	(B)	(B)
(E) Rescue robot (Tsukagoshi et al. 2005)	2300	15	80	unknown	0.03	5.3	(C)	(A)
EPFL jumping robot (presented here)	**14**	**18**	**62**	**46**	**4.17**	**3.4**	**(C)**	**(D)**

marizes the size, weight and performance values of these robots.

In comparison to these existing systems, our robot is one order of magnitude lighter and can jump much higher for its weight, which favors its applicability in situations such as space exploration, where low weight is of supreme importance (Yim et al. 2003). In order to design this robot, we proceed by separating the desired behavior in three functions, i.e. jumping, uprighting and steering. We then evaluate existing designs and extract the basic method for doing the tasks, compare them using a weighted evaluation procedure and propose a novel way to achieve the behavior. Our main design requirement is to keep structural simplicity and robustness at a low mass of our system. Further, we describe the design details and integration of these three functions into one working prototype. As a characterization of the jumping performance of our robot we characterize and discuss the 'cost' of the ability to upright and steer. We also explain and characterize how the jumping height and the jumping distance can be altered by changing the configuration of the robot. Finally, we demonstrate the remote controlled prototype moving successfully and repetitively over an obstacle course. High-speed video footage of its behavior can be seen in the accompanying video material (video 1–4) and at http://lis.epfl.ch/microglider.

2 Design Methodology

In order to design our robot capable of performing steered repetitive jumps, we divided the required functionality into three functions, i.e. jumping, uprighting and steering and applied the engineering design process as described in Ullman (2002). The sequential steps in this design process are (i) the conceptual design of the principles needed to fulfill the predefined functions, (ii) their comparison using a weighted comparative evaluation method, (iii) their implementation in a computer aided design (CAD) software and finally (iv) their fabrication and assembly.

In the following section we will present and explain the principles of jumping, uprighting and steering. As the main focus of this article is on how to achieve uprighting and steering for jumping robots, we will first describe briefly the principle of the jumping mechanism that we used as propulsion unit for our robot and then proceed to assess how to provide it with the ability to upright and steer. For the uprighting and steering we will analyze the principles that are implemented in existing robots and add one additional method for steering that has not been presented before. We will then compare them based on our design requirements.

In order to allow the robot to jump high, the weight of the entire system should be kept as low as possible. We therefore choose the first design requirement to be a minimization

of the mass of our robot. As a second design requirement we want to keep the structure as simple as possible to ease manufacturing and assembly. The third requirement is to build the mechanism as robustly as possible to minimize the risk of mechanical failure. The fourth and final requirement is to minimize energy consumption for performing the different functions, as this would reflect in a need for bigger and heavier batteries which would again decrease the jumping height. Based on these four design requirements, we will decide which principles to implement in our robot.
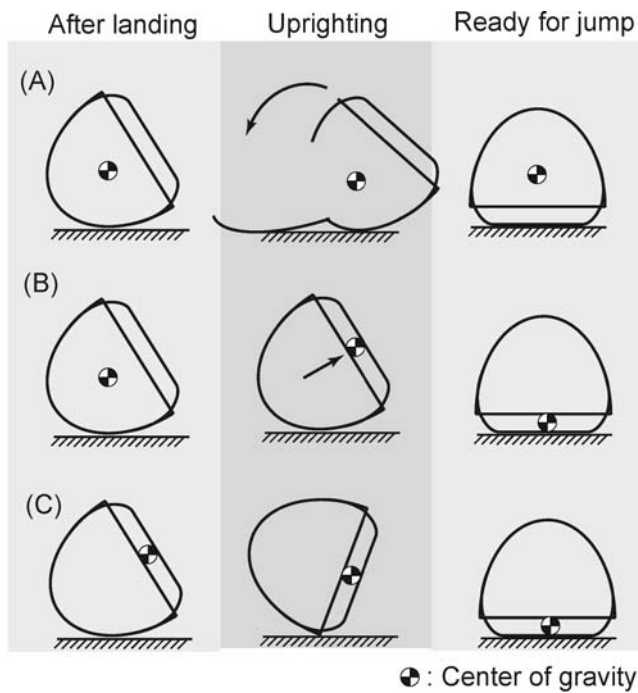
2.1 Jumping Mechanism

The main requirement in the development of the jumping mechanism is to build a lightweight propulsion unit for jumping robots, where the jumping height and take-off angle can be adjusted. For small jumping systems it is most beneficial to first slowly charge an elastic element and then use the legs as a catapult to jump (Roberts and Marsh 2003; Alexander 1988; Burrows 2003; Scarfogliero et al. 2007; Kovac et al. 2008). This way of jumping is used by small animals such as desert locusts (Bennet-Clark 1975), fleas (Gronenberg 1996) and frogs (Roberts and Marsh 2003). The working principle in our design is to first charge a torsion spring and then release its energy to quickly extend a four bar leg linkage to perform the jumping movement, as illustrated in Fig. 3. This same principle has been implemented for our previously presented minimalist jumping robot (Kovac et al. 2008). The basic components are the four bar leg mechanism that is connected to the body on the ground link (a) and is actuated via the input link (b) using a torsion spring (c).

2.2 Uprighting Mechanism

We classify the uprighting mechanisms of the existing robots in three categories of principles on how to achieve
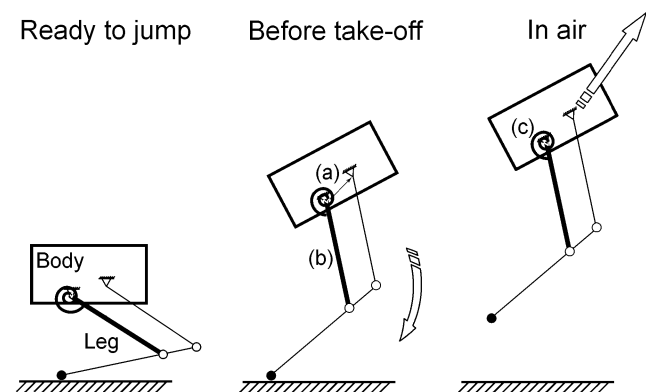
Fig. 3 Working principle for the jumping mechanism. In order to jump, a four bar leg linkage that is attached to the body on the ground link (**a**) is extended quickly via the input link (**b**) using a torsion spring (**c**)

Fig. 4 Three working principles for uprighting. (**A**) Arms or levers are moved actively after landing, (**B**) the center of gravity is actively shifted after landing to upright, (**C**) the position of the center of gravity leads to a passive uprighting movement

Table 2 Weighted evaluation of the three working principles for the uprighting mechanism (Fig. 4)

Criteria	Weight	(A)	(B)	(C)
Light weight	0.4	4	3	**4**
Simplicity	0.1	1	3	**5**
Robustness	0.2	2	3	**4**
Energy consumption	0.3	1	2	**5**
Total	1	2.4	2.7	**4.4**

1: very unfavorable – 5: very favorable

The third and final principle on the uprighting mechanism (Fig. 4.C) as it is implemented in the "Sandia robot" (Fig. 2.A) is a completely passive mechanism where the center of gravity is located in the lower part of the structure and creates a roll momentum to upright the robot. Compared to the second solution it is more effective because on landing and bouncing on the ground it already has the strong tendency to settle in an upright position. Since it does not need actuators and moving parts, it is a very simple, robust and energetically cheap solution. We therefore choose this principle to achieve the uprighting for our robot.

2.3 Steering Mechanism

We can classify the steering principles of the existing robots in four categories and compare them using the same weighted comparative evaluation (Ullman 2002) (Table 3). The first principle (Fig. 5.A) uses wheels to turn the robot, such as in the case of the "scout robot" (Fig. 2.B) and the "rescue robot" (Fig. 2.E). It is a simple solution, but not very effective in cases where the terrain is not smooth because even small obstacles may prevent it from turning. In addition, it requires structures external to the robot that are exposed to potential damage on landing.

The principle (B), as used on the "Sandia robot" (Fig. 2.A) and *Jollbot* (Fig. 2.D) consists of shifting the center of gravity and consequently changing the direction of the jump. Card and Dickinson showed recently (Card and Dickinson 2008) that Drosophila flies use this same principle to direct their escape jump. The advantage of this solution is that the actuation is inside the structure and therefore it is less prone to damage and more robust compared to the principle (A). The energy consumption is relatively low as only a fraction of the robot weight has to be moved and not the entire structure. The main drawback however, is that it is less effective compared to other principles where the entire robot is oriented prior to jumping because the shifting of the center of gravity can only change the lateral take-off angle. Another potential drawback is that shifting the position of the center of gravity affects the mass distribution of the structure and therefore also changes the in air behavior of the robot. This

the uprighting movement (Fig. 4) and compare them using a weighted comparative evaluation (Ullman 2002) (Table 2). The first principle (A) consists of using arms or levers that are moved actively after landing to upright the structure, as it is implemented in the "minimalist jumping robot" (Fig. 2.C). It is conceptually similar to the active uprighting of insects as described in Faisal (2001) and Frantsevich (2004). This principle offers the advantage of being able to accomplish the uprighting movement on smooth surfaces as well as on rough terrain where the uprighting movement may be obstructed. Compared to the other solutions, it is thus very effective. Its drawback however is that it requires additional actuators and a certain amount of energy to lift the entire structure and perform the movement. These additional actuators and hinges increase the complexity of the system and potentially decrease its mechanical robustness by making the entire system more error prone.

The second principle (Fig. 4.B) consists of moving a mass that is internal to the structure in order to create a roll momentum and upright the system as it is implemented in *Jollbot* (Fig. 2.D). It is a fairly simple, effective and robust solution, but it has the shortcoming that the robot after landing first settles in an upside down position and only then, an actuator shifts the weight at a certain energy cost. It carries the risk that the robot can be stuck in case that the terrain is not smooth enough and the rolling moment due to the weight shift is not sufficient to overcome the obstruction.

Table 3 Weighted evaluation of the four different working principles for the steering mechanism (Fig. 5)

Criteria	Weight	(A)	(B)	(C)	**(D)**
Light weight	0.4	3	2	4	**5**
Simplicity	0.1	5	3	2	**2**
Robustness	0.2	2	4	4	**5**
Energy consumption	0.3	3	4	3	**4**
Total	1	3	3.1	3.5	**4.4**

1: very unfavorable – 5: very favorable

either leads to uncontrolled tumbling in air which decreases the jumping performance or it calls for a control strategy which then again increases the complexity of the system.

In the principle (C), as it is implemented in the "minimalist jumping robot" (Fig. 2.C), the entire system turns on a foot. Its main drawback is that in order to turn, the foot must be in contact with the ground and the rest of the structure free to turn, which may be unlikely when the ground is uneven.

In addition to these three existing working principles for steering, we propose the principle (D) which, to the best of our knowledge, has never been implemented for steered jumping. It is similar to the principle (C) only that the foot is lifted and turned inside the structure. This simple way of orienting the robot combines the effectiveness of turning it prior to jumping such as solution (A) and (C) with the robustness to encapsulate the jumping mechanism inside the structure such as in solution (B). We therefore implement the working principle (D) in our jumping robot.

3 Implementation

The next step in the development of our jumping robot is to implement the chosen working principles for jumping, up-righting and steering in CAD, integrate the subsystems, fabricate the components and assemble the prototype (Fig. 6). In this section, we describe how we implemented the chosen principles and illustrate the design details of our jumping robot.

3.1 Jumping Mechanism

The jumping mechanism (Fig. 7) is a further development of our previously presented minimalist jumping robot (Kovac et al. 2008). As described in Sect. 2.1 the basic principle is to charge a torsion spring and release its energy to extend a four bar leg linkage to jump (Fig. 3). We use a 4 mm DC motor (a) to turn an eccentric cam (b), similar to the one in Scarfogliero et al. (2007). The motor turns the cam in counterclockwise direction, by way of a four stage gear box (c),
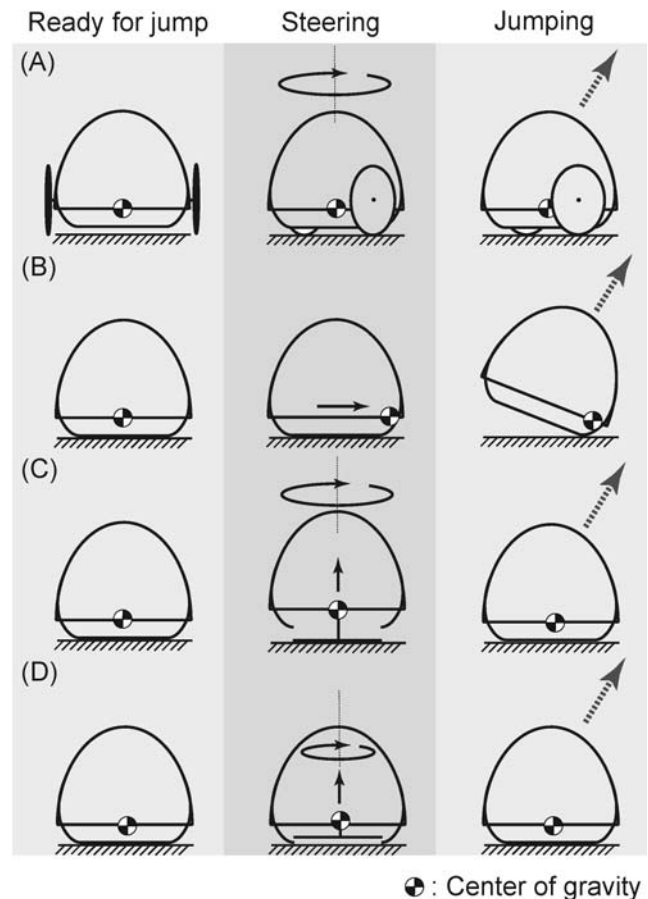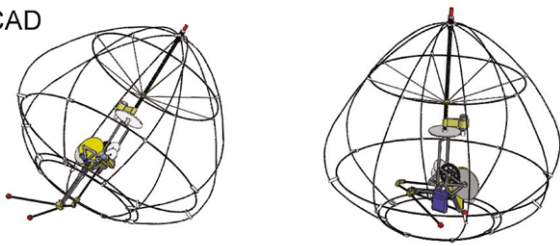

Fig. 5 Four working principles for steering of the robot. (**A**) Wheels allow rotation on the spot prior to jumping, (**B**) center of gravity shifting to change the take-off direction, (**C**) a foot rotates the robot before jumping, (**D**) the jumping mechanism is rotated inside of the cage before jumping

in order to charge two torsion springs (d). These two springs are located around the axis of the leg (e) and are fixed to the frame (f) and the main leg (g). Once the most distal point of the cam is reached, the energy that is stored in the springs actuates the main leg which is the input link for the four bar leg mechanism. The jumping height, take-off angle and ground force profile can be adjusted by changing the spring setting (h) and the geometry of the legs (Kovac et al. 2009b). A jump can be executed every 3 s with a power consumption of 350 mW. The reader may be referred to Kovac et al. (2008) for a more detailed explanation and characterization of the jumping principles used.

The materials used are aluminum 7075 for the frame and the main leg, carbon prepreg rods for the legs, Poly-oxymethylene plastic (POM) for the gears and cam and polyaryletheretherketone (PEEK) for the connection pieces on the legs and the frame. The properties of the different materials are summarized in Table 4.

The difference of this jumping mechanism compared to the system presented in Kovac et al. (2008) is that it is more
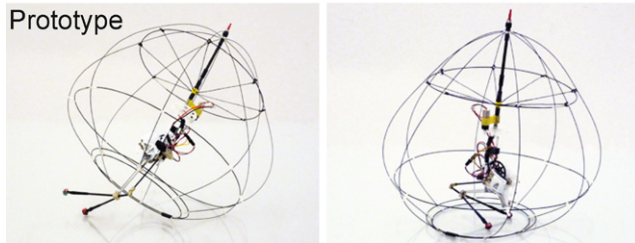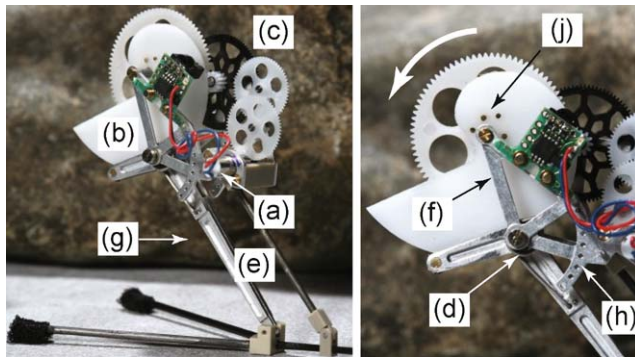
Fig. 6 Jumping robot CAD design and fabricated prototype. We choose the design principle (Fig. 4.C) for the uprighting and (Fig. 5.D) for the steering of the robot

Fig. 7 Jumping mechanism that presents the propulsion unit for our robot. (**a**) 4 mm DC pager motor, (**b**) cam, (**c**) four stage gear box, (**d**) two steel torsion springs, (**e**) four bar linkage leg structure, (**f**) aluminum frame, (**g**) main leg as input link, (**h**) spring setting, (**j**) fixation of the cam to the last gear stage using five bolts

robust and allows for a better jumping performance. The frame is fabricated of aluminum instead of Cibatool and is therefore lighter, more stable and has a better guidance for the axes of the gears. In order to increase robustness of the connection between the cam and the last gear stage we use now five bolts (j) instead of only two that were very close to the axis of the cam. Compared to the previous design it also offers a higher spring setting (h) to regulate the jumping height. Summarizing, the jumping mechanism has the same weight but is much more robust than the system presented in Kovac et al. (2008).

3.2 Uprighting Mechanism

The uprighting mechanism consists of a cage structure designed so that it passively rolls into a position suitable for the next jump (Fig. 8). The carbon axis (a) is connected to

Table 4 Properties of the materials used

	Alu 7075	PEEK	POM	Carbon prepreg	ABS plus
Density [g/cm^3]	2.7	1.3	1.56	1.55	1.04
E-Module [GPa]	69	3.5	5.2	130	2.2
Yield strength [MPa]	320	97	62	1400	53

eight vertical 0.5 mm carbon rods (b) and four horizontal 0.7 mm carbon rings (c) using rigid joints (d), (e), (f), (g) to hold them together. The jumping mechanism (h) is attached within the cage on the axis using an aluminum fork (i). In order to reinforce the entire structure we added eight wires (k) that hold the axis to the first horizontal carbon ring.

The materials used for the cage are commercially available carbon rods connected through rigid joints printed out of ABS plus.
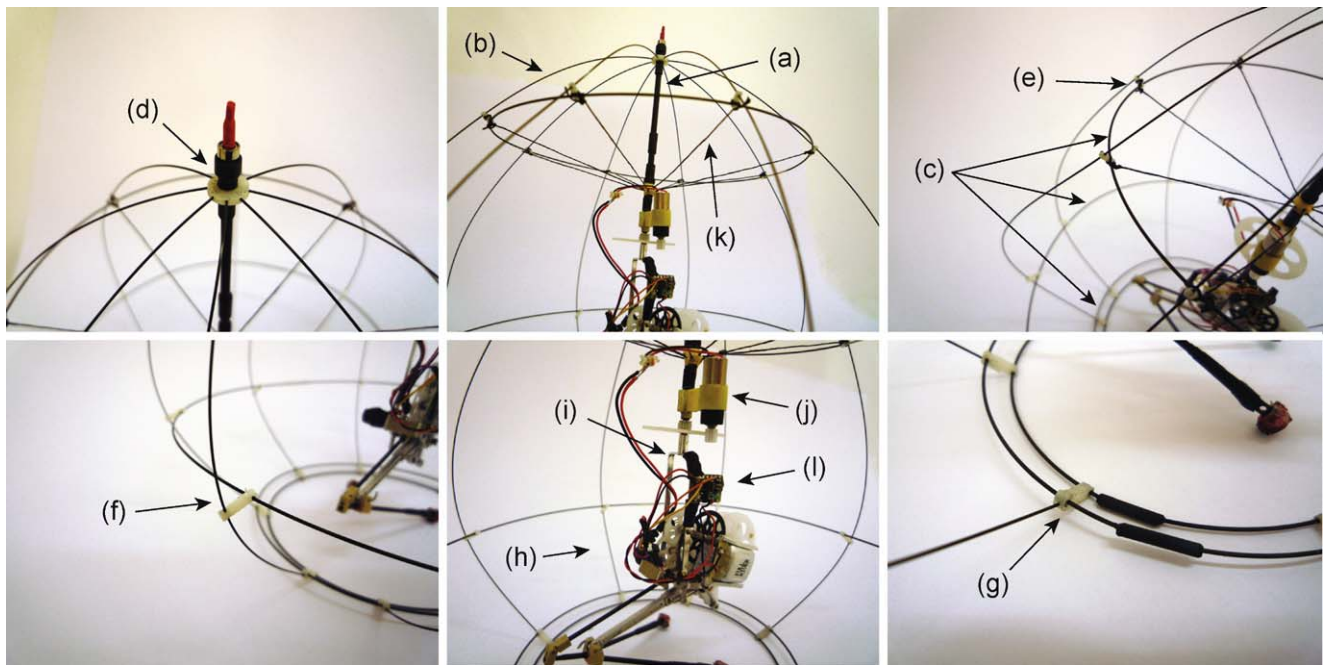
3.3 Steering Mechanism

The turning of the jumping mechanism inside the cage around the axis is realized using a motor and a double guided axis (Fig. 9). The 1.5 mm carbon tube (a) is connected to the cage on the top connection piece (b) and guides a 1 mm carbon rod (c) which can rotate freely around its axis. A 6 mm DC motor with inbuilt 1/25 gearbox (d) which is fixed to the carbon tube (a) drives a module 0.3 12/81 teeth gear (e) which is fixed to the carbon rod (c) and the fork (f) that holds the jumping mechanism. In order to keep the axial position and to reduce friction between the carbon tube (a) and the carbon rod (c), a 1.5 mm ball bearing (g) is added as interface. The transmission ratio from the motor to the axis is 1/225 in order to allow a slow enough rotation of the axis of 35.5 rotations per minute at a motor speed of 8000 rotations per minute.

3.4 Integration

After landing and rolling, the jumping mechanism charges for the next jump and the cage passively uprights until the only contact with the ground is the base of the cage (Fig. 10). The duration of the entire uprighting movement takes 2 s. Once upright, the entire jumping mechanism is inside of the cage and can rotate around its vertical axis as illustrated in Fig. 9. The take-off sequence takes 18 ms from touching the ground with the feet until the robot leaves the ground with a take-off velocity of 3.47 m/s (Fig. 11).

In order to reduce the risk of damaging the legs on landing, the charging of the jumping mechanism starts already during the aerial phase to better protect the legs inside of

Fig. 8 Mechanical design details of the jumping robot. (**a**) axis of the robot, (**b**) 0.5 mm carbon rods, (**c**) 0.7 mm carbon ring, (**d**), (**e**), (**f**), (**g**) connection pieces to hold the carbon ring and carbon rods together, (**h**) jumping mechanism as propulsion unit of the robot, (**i**) aluminum fork to interface the axis of the robot to the jumping mechanism, (**j**) 6 mm DC pager motor to rotate the jumping mechanism around the axis, (**k**) wires to reinforce the cage structure, (**l**) 3-channel remote control
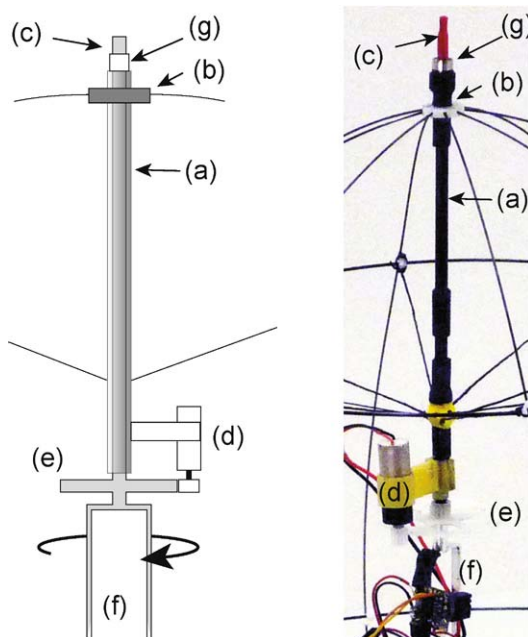
Fig. 9 Implementation of the steering mechanism. (**a**) 1.5 mm carbon tube, (**b**) connection piece, (**c**) 1 mm carbon rod, (**d**) 6 mm DC pager motor with inbuilt 1/25 gearbox, (**e**) module 0.3 12/81 teeth gear, (**f**) aluminum fork, (**g**) 1.5 mm ball bearing

Table 5 Weight budget of the prototype

Part	Mass [g]
Total mass jumping mechanism	6.87
Carbon cage and axis	3.79
Motor with transmission	2.24
Remote control	0.70
LiPo Battery 10 mA h	0.73
Total mass prototype	**14.33**

The position of the center of gravity is located 5.2 cm above the base of the cage when the legs are extended and 5.3 cm when the legs are contracted. Its position in the lower part of the cage ensures a passive uprighting after landing.

The motor to steer and the motor of the jumping mechanism are remotely controlled using a miniature DIDEL 3-channel infra red controller (Fig. 8.l) with a mass of only 0.7 g. The battery used is a FullRiver 10 mA h Lithium Polymer battery with a operating voltage of 3.7 V. The 10 mA h provided by this battery would thus theoretically allow for 6.3 min of continuous recharging of the jumping mechanism or approximately 108 jumps.

The completely functional remote controlled prototype has a total size of 18 cm and a mass of 14.33 g including batteries and electronics (weight budget in Table 5).

the cage. As the center of gravity is in the lower part of the structure, the robot settles in a stable upright position and is ready to steer and jump again (see accompanying video 1).
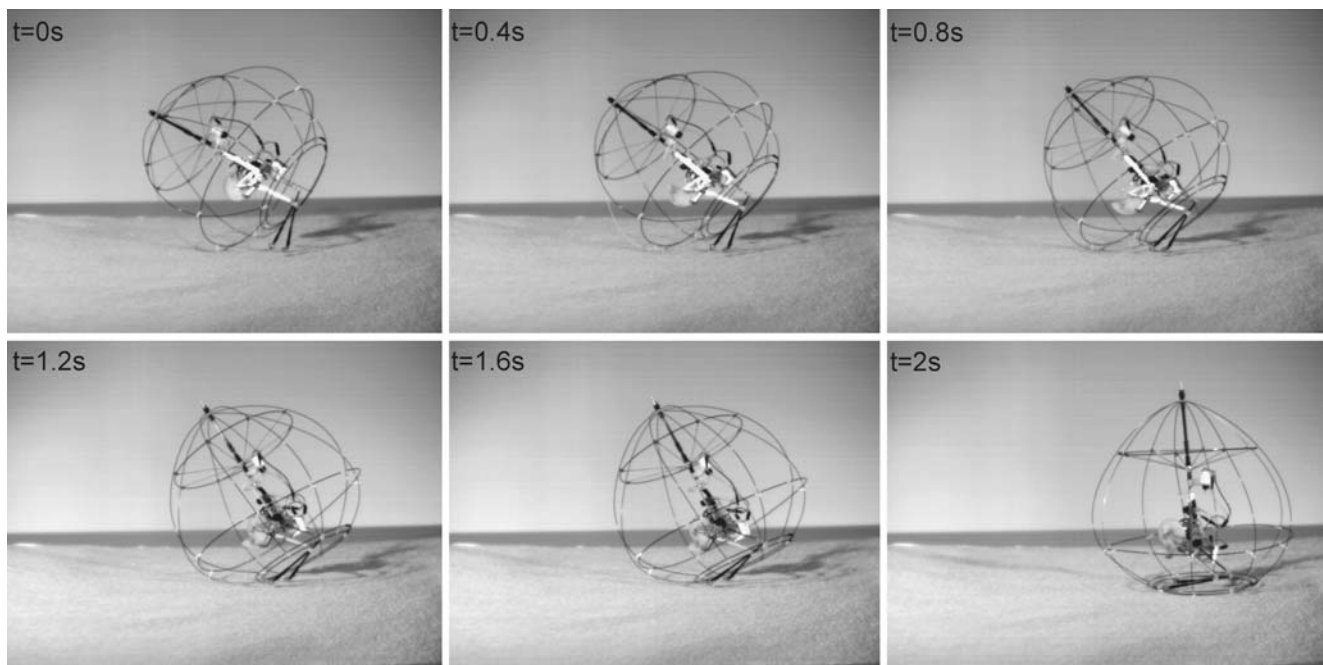
Fig. 10 Uprighting sequence after landing and charging for the next jump. The center of gravity of the entire structure is in the lower part of the cage so that the robot uprights passively. When the jumping mech-anism charges for the next jump, the legs are retracted within the cage in 2 s. After this, the jumping mechanism is free to rotate around its vertical axis inside of the cage and jump (see accompanying video 1)
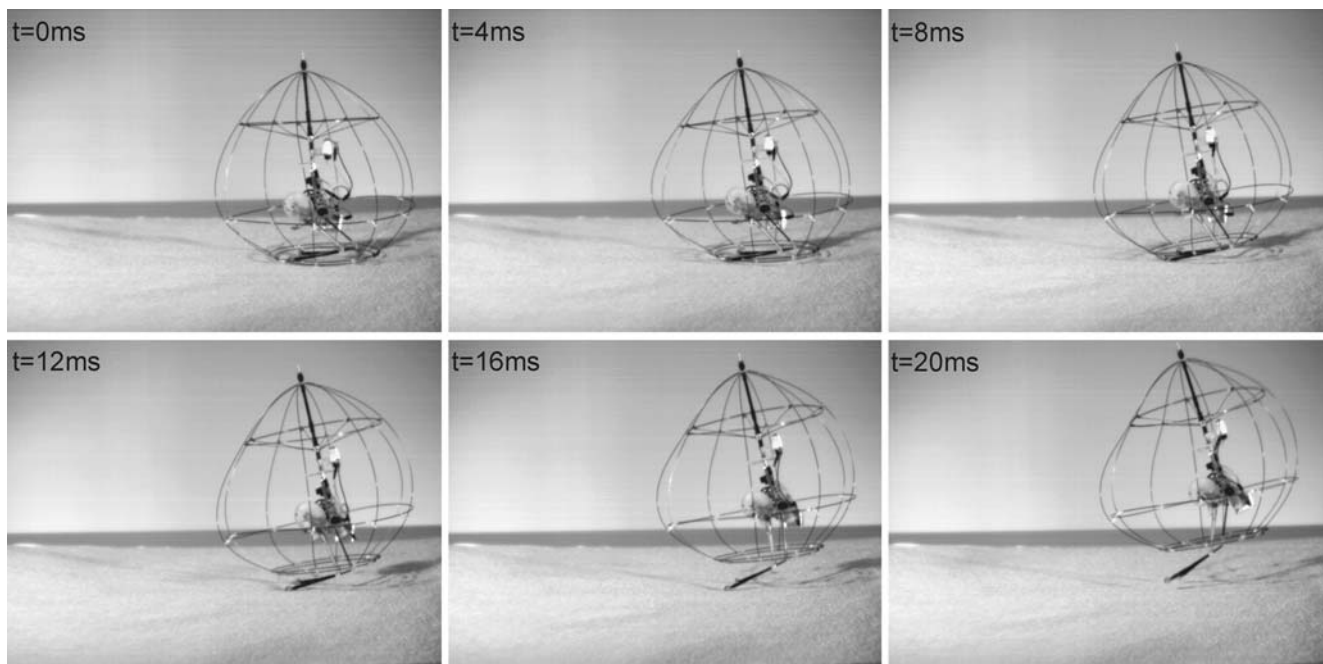

Fig. 11 Take-off sequence. The take-off velocity of 3.47 m/s is reached in 18 ms (see accompanying video 1)

3.5 Adjustment of the Jumping Parameters

Depending on the terrain where the robot is supposed to operate in, different configurations of the jumping robot may be optimal. For locomotion in an environment where the obstacles are relatively high compared to the robot size, the take-off angle and jumping height should be higher than in flat terrain. In order to address these needs for a mission de-
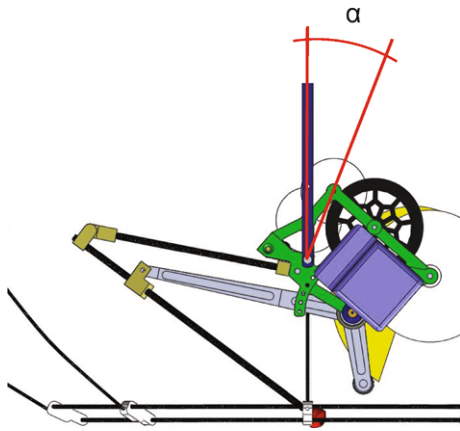
Fig. 12 Integration of the jumping mechanism with the cage. The jumping distance can be changed by adjusting the angle α which positions the attitude of the jumping mechanism inside of the cage

pendent adjustment of the jumping robot, we implemented several ways how to adjust the jumping height and the jumping distance.

The jumping height can be adjusted by choosing a different pre-load angle for the torsion springs (Fig. 7.h) as characterized in Kovac et al. (2008). The take-off angle and consequently the jumping distance can be adjusted by altering the attitude of the jumping mechanism inside of the cage (angle α in Fig. 12).

4 Results

In order to characterize the performance of the robot, we performed a series of experiments to determine the jumping height, take-off angles and jumping distance, depending on the different settings of the jumping robot. The durations, velocities and trajectories are measured optically, using a TroubleShooter 1000 high-speed camera system at 500 frames per second and ProAnalyst, an adequate motion analysis software.

4.1 The Cost of the Cage

The goal of this first set of experiments is to estimate how much the jumping height is reduced due to the addition of the uprighting and steering ability to the jumping mechanism. We measure the jumping trajectory of the jumping robot for the complete robot prototype with cage, the robot without cage but the same weight as the caged system, and finally the jumping mechanism only, without cage. For every configuration we perform one jump and plot the jumping trajectory in Fig. 13. The first jumping trajectory is performed by the jumping robot with cage and a total mass of 14.33 g. At a take-off angle of 75° it jumps a height of 62 cm. The second trajectory is performed by the jumping mechanism
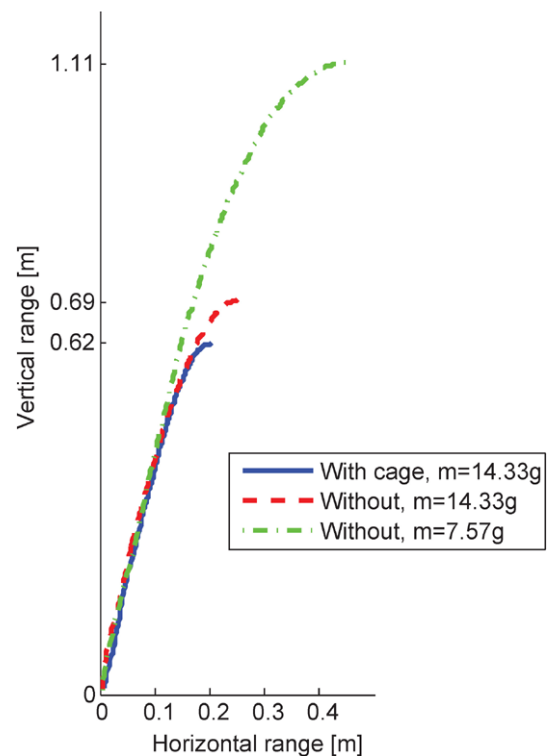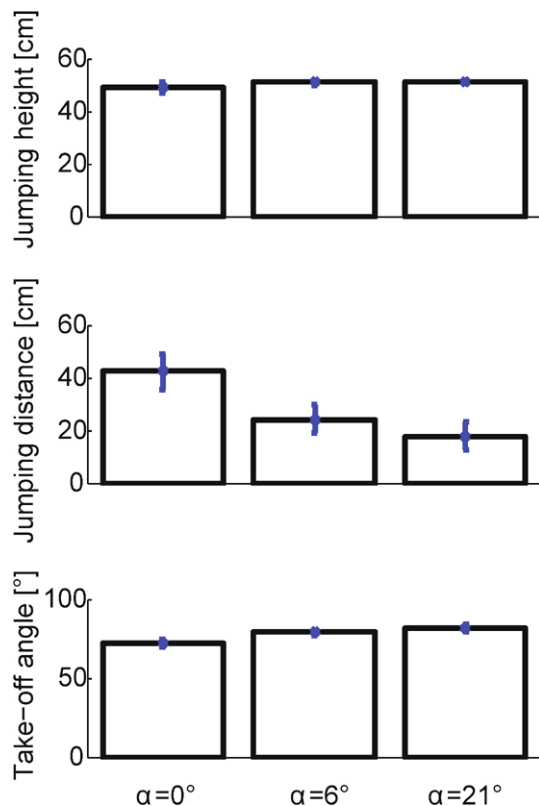

Fig. 13 Jumping trajectory of the jumping robot for the complete robot prototype with cage, the robot without cage but the same weight as the caged system, and the jumping mechanism only, without cage. With the cage as a fully functional prototype it can jump a height of 62 cm and a distance of 46 cm at a take-off angle of 75° (see accompanying video 2)

with a payload of 6.76 g to simulate the weight of the cage. In this configuration it jumps a height of 69 cm at a take-off angle of 75°. The third trajectory is performed by the jumping mechanism with only the remote control and battery and without the cage. In this configuration the robot has a mass of 7.57 g and jumps a height of 111 cm at a take-off angle of 75°. For high speed video footage of these jumps, see the accompanying video 2.

4.2 Adjustment of the Jumping Parameters

In this set of experiments we characterize the change of jumping distance for three different settings of the angle α, i.e. 0°, 6° and 21° (Fig. 12) which positions the attitude of the jumping mechanism inside the cage. For each of these three configurations we perform five jumps and compare the average jumping height, average jumping distance and the average take-off angle (Fig. 14). The average jumping distance for $\alpha = 0°$ is 42.2 cm at an average take-off angle of 71.7°. The average jumping distance for the configuration with $\alpha = 6°$ is 24.2 cm at an average take-off angle of 78.6°. For the third configuration with $\alpha = 21°$, the robot jumps an average distance of 17.8 cm at an average take-off angle

Fig. 15 Trajectory of the jumping robot successfully climbing two stairs of each 50 cm height and jumping into a window. The accompanying video 4 shows the behavior of three subsequent successful passages of this obstacle course
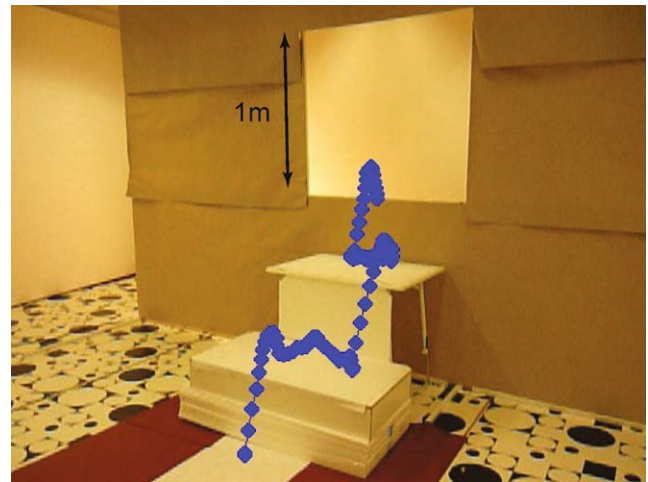
Fig. 14 Average values and standard errors for the jumping height, the jumping distance and the take-off angle for $\alpha = 0°$, $\alpha = 6°$, $\alpha = 21°$ (Fig. 12)

of 81.7°. In order to analyze if the jumping heights, jumping distances and take-off angles are different, we perform a Kruskal-Wallis test (Hollander and Wolfe 1999). The jumping distance is significantly different ($df = 14$, $p < 0.01$), the take-off angle as well is significantly different ($df = 14$, $p < 0.05$), and the jumping height is not significantly different ($p = 0.087$) for the three configurations of the robot (Fig. 12, $\alpha = 0°$, 6°, 21°). For high speed video footage of these jumps, see the accompanying video 3.

4.3 Locomotion on an Obstacle Course

As a demonstration to show the ability of our jumping robot prototype to successfully perform steered jumps in cluttered environments, we built an obstacle course in our laboratory which consists of two stairs with a height of 45 cm each and a window of 1 m × 1 m (Fig. 15). We place the robot on the ground at 10 cm distance to the first stair and aim at jumping with several sequential steered jumps upstairs and into the window, all without human intervention on the scene. Depending on the operating skill of the human operator the window can be entered in approximately four jumps (see the accompanying video 4 for three successful passages of this obstacle course). For a better overview of the obstacle course, we depict the trajectory of only one successful run

in Fig. 15. This demonstration summarizes the achieved design goals and successful locomotion ability of our jumping robot in cluttered environments.

5 Discussion

Compared to the jumping mechanism only, the mass increase of 6.76 g for the cage reduces the jumping height by 38% from 111 cm to 69 cm. By adding the actual cage structure it is reduced further by 7 cm. This additional decrease in jumping height is due to the higher aerodynamical friction during jumping and the fact that the cage experiences oscillations right after take-off (see accompanying movie 1), which is lost energy that can not be converted into jumping height. The 'cost' of having the ability to upright on landing and being able to steer for our current robot corresponds therefore to a decrease in jumping height of 44% compared to the jumping robot mechanism without those abilities.

The jumping height of our robot could be increased by reducing the weight of the cage, e.g. using a smaller motor to turn the jumping mechanism inside the cage, or by increasing the structural stiffness of the cage to reduce the oscillations after take-off. However, using carbon rods as the structural material for the cage, it may be very difficult to further increase the stiffness of the cage without adding much additional material, which then again would decrease the jumping height due to the additional weight. Further research could address this trade-off.

The results of the experiments for the adjustment of the jumping parameters indicate that the jumping distance and the take-off angle are different for the three settings of α ($p < 0.01$ for the jumping distance and $p < 0.05$ for the

take-off angle). As an extension of the current system, a next generation of the jumping robot could be able to adapt the take-off angle and jumping distance prior to every jump by actuating the attitude of the jumping mechanism inside the cage (Fig. 12) using a small DC motor or a shape memory alloy actuator (Kovac et al. 2007).

The main benefits that our jumping robot offers compared to other existing jumping robots is the ability to successfully move in cluttered environments at a very low weight. The low weight has the advantages that (i) the robot consumes less energy to locomote compared to bigger and heavier systems, (ii) that the impact forces are lower when landing and (iii) that it could be employed in missions such as space exploration where the weight of the systems carried into space is a major constraint (Yim et al. 2003).

The main limitation of our current robot is a payload of only a few grams in order to be still able to jump a reasonable height of several times its own size. It is thus rather suited for low weight and low energy sensors and communication devices. For example, an electronic board populated with a microcontroller, a three axis accelerometer, a Hall sensor on the cam and an H-bridge motor driver as described in Kovac et al. (2009a) has a weight of only 1.3 g. Already this minimal electronic setup would allow the robot to detect its orientation and cam charging state and perform repetitive jumps autonomously. Adding two linear cameras with rate gyros could enable it additionally to avoid obstacles using optical flow at an additional mass of only 1.8 g (Zufferey et al. 2007).

Depending on the desired task that this jumping robot platform is supposed to fulfill, other sensors could be added as well. If needed, it could be scaled up to be able to carry higher payloads. However, designing the robot to carry higher payloads would require its structure to be more robust as the impact forces on landing increase linearly with the mass of the system. There may thus be a trade-off between possible payload of the robot and its own weight. Further research will address scaling issues of this robot in order to optimize trade-offs between payload and weight of the system.

6 Conclusion

We presented the development and characterization of a working jumping robot prototype with a mass of 14 g that can perform repetitive steered jumps with a height of up to 62 cm at a take-off angle of 75°. As a demonstration of the achieved design goals and its locomotion ability, we showed it repetitively moving over an obstacle course where it has to consecutively jump two stairs of 45 cm height each and jump through a window (see accompanying videos 1–4). Its low weight and the adjustability of the jumping height and jumping distance make it a suitable robotic platform for applications such as environmental monitoring or space exploration.

References

Alexander, R. M. (1988). *Elastic mechanisms in animal movement*. Cambridge: Cambridge University Press.
Alexander, R. M. (2003). *Principles of animal locomotion*. Princeton: Princeton University Press.
Armour, R., Paskins, K., Bowyer, A., Vincent, J. F. V., & Megill, W. (2007). Jumping robots: a biomimetic solution to locomotion across rough terrain. *Bioinspiration and Biomimetics Journal*, *2*, 65–82.
Bennet-Clark, H. C. (1975). The energetics of the jump of the locust *Schistocerca gregaria*. *Journal of Experimental Biology*, *63*(1), 53–83.
Brackenbury, J., & Hunt, H. (1993). Jumping in springtails: mechanism and dynamics. *Journal of Zoology*, *229*, 217–236.
Burdick, J., & Fiorini, P. (2003). Minimalist jumping robot for celestial exploration. *The International Journal of Robotics Research*, *22*(7), 653–674.
Burrows, M. (2003). Biomechanics: Froghopper insects leap to new heights. *Nature*, *424*(6948), 509.
Card, G., & Dickinson, M. (2008). Performance trade-offs in the flight initiation of drosophila. *Journal of Experimental Biology*, *211*(3), 341.
Faisal, A. (2001). Coordinated righting behaviour in locusts. *Journal of Experimental Biology*, *204*(4), 637–648.
Frantsevich, L. (2004). Righting kinematics in beetles (insecta: Coleoptera). *Arthropod Structure and Development*, *33*(3), 221–235.
Gronenberg, W. (1996). Fast actions in small animals: springs and click mechanisms. *Journal of Comparative Physiology A: Sensory, Neural, and Behavioral Physiology*, *178*(6), 727–734.
Hollander, M., & Wolfe, D. A. (1999). *Nonparametric statistical methods*. New York: Wiley.
Kaspari, M., & Weiser, M. D. (1999). The sizegrain hypothesis and interspecific scaling in ants. *Functional Ecology*, *13*(4), 530–538.
Kovac, M., Guignard, A., Nicoud, J. D., Zufferey, J. C., & Floreano, D. (2007). A 1.5 g sma-actuated microglider looking for the light. In *IEEE international conference on robotics and automation*, pp. 367–372.
Kovac, M., Fuchs, M., Guignard, A., Zufferey, J., & Floreano, D. (2008). A miniature 7 g jumping robot. In *IEEE international conference on robotics and automation*, pp. 373–378.
Kovac, M., Schlegel, M., Zufferey, J. C., & Floreano, D. (2009a). A miniature jumping robot with self-recovery capabilities. In *IEEE/RSJ international conference on robotics and automation*, pp. 583–588.
Kovac, M., Zufferey, J., & Floreano, D. (2009b). Towards a self-deploying and gliding robot. In Floreano, D., Zufferey, J. C., Srinivasan, M. V., & Ellington, C. (Eds.), *Flying insects and robots* Berlin: Springer, Chap. 19.
Lambrecht, B. G. A., Horchler, A. D., & Quinn, R. D. (2005). A small, insect-inspired robot that runs and jumps. In *IEEE/RSJ international conference on robotics and automation*, pp. 1240–1245.
Roberts, T. J., & Marsh, R. L. (2003). Probing the limits to muscle-powered accelerations: lessons from jumping bullfrogs. *Journal of Experimental Biology*, *206*(15), 2567–2580.

Scarfogliero, U., Stefanini, C., & Dario, P. (2007). Design and development of the long-jumping "grillo" mini robot. In *IEEE international conference on robotics and automation*, pp. 467–472.

Stoeter, S. A., Rybski, P. E., & Papanikolopoulos, N. (2002). Autonomous stair-hopping with scout robots. In *IEEE/RSJ international conference on intelligent robots and systems*, Vol. 1, pp. 721–726.

Sugiyama, Y., Yamanaka, M., & Hirai, S. (2005). Circular/spherical robots for crawling and jumping. In *IEEE international conference on robotics and automation*, pp. 3595–3600.

Tsukagoshi, H., Sasaki, M., Kitagawa, A., & Tanaka, T. (2005). Design of a higher jumping rescue robot with the optimized pneumatic drive. In *IEEE international conference on robotics and automation*, pp. 1276–1283.

Ullman, D. G. (2002). *The mechanical design process*. New York: McGraw-Hill.

Weiss, P. (2001). Hop... hop... hopbots!: designers of small, mobile robots take cues from grasshoppers and frogs. *Science News*, *159*, 88.

Yim, M., Roufas, K., Duff, D., Zhang, Y., Eldershaw, C., & Homans, S. (2003). Modular reconfigurable robots in space applications. *Autonomous Robots*, *14*(2), 225–237.

Zufferey, J. C., Klaptocz, A., Beyeler, A., Nicoud, J. D., & Floreano, D. (2007). A 10-gram vision-based flying robot. *Advanced Robotics*, *21*(14), 1671–1684.

Mirko Kovač is Ph.D. candidate at the Laboratory of Intelligent Systems within the School of Engineering at Ecole Polytechnique Fédérale de Lausanne (EPFL). He received his M.S. degree in Mechanical Engineering from the Swiss Federal Institute of Technology in Zurich (ETHZ) in 2005 with his master thesis carried out at University of California in Berkeley, USA. During his studies he was research associate with RIETER Automotive Switzerland, the WARTSILA Diesel Technology Division in Switzerland, and Ciserv in Singapore. He has presented his work on several international conferences and journals and has supervised 20 B.A./M.S. level student projects. In 2009, he received a best paper award at the International Conference on Robotics and Intelligent Systems (IROS'09). His research interest is the conception and design of novel locomotion and control methods for mobile robots and its analogy in biological systems.
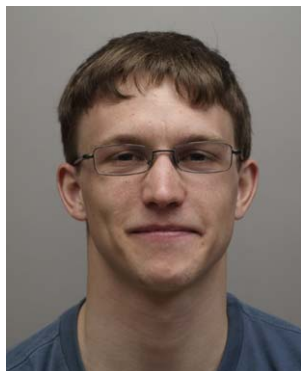
Manuel Schlegel is currently master student in robotics at Ecole Polytechnique Fédérale de Lausanne (EPFL). In 2008 he received the B.S. degree in Microengineering from the EPFL. In parallel to his studies he is research assistant at the Laboratory of Intelligent Systems within the School of Engineering at EPFL where he worked on the design and prototyping of several miniature jumping robots. His research interest is the conception and fabrication of smart structures for the use in miniature mobile robots.

Jean-Christophe Zufferey is group leader at the Laboratory of Intelligent Systems and lecturer in mobile robotics. In 2001 he obtained a Master in micro-engineering from EPFL with a research project carried out at Carnegie Mellon University and in 2005 a Ph.D. in flying robotics from EPFL, for which he received the ABB best Ph.D. award. He is author or co-author of more than 30 peer-reviewed publications, among which a book on Bio-inspired Flying Robots (2008) by the EPFL Press being distributed worldwide by CRC Press. He received the 2006 best paper award at the International Conference on Robotics and Intelligent Systems. In 2007, he co-organized the first international symposium on Flying Insects and Robots with over 100 participants. He is currently coordinating a team of six Ph.D. students working in the design, prototyping, control, and coordination of several small flying platforms equipped with miniature and low-power sensing capabilities. Jean-Christophe is also co-founder of two spin-offs from EPFL.

Dario Floreano is Director of the Laboratory of Intelligent Systems within the School of Engineering at Ecole Polytechnique Federale de Lausanne (EPFL). He received an M.A. in Cognitive Science from University of Trieste (Italy) in 1988, an M.S. in Neural Computation from the University of Stirling (UK) in 1991, and a Ph.D. in Evolutionary Robotics in 1995 from University of Trieste (Italy), all of them with distinction. In 1996 he was appointed senior researcher at the Department of Computer Science of EPFL where he established the Robot Learning group. In 1998 he was invited researcher at Sony Computer Science Labs in Tokyo. In 2000 he was awarded a Swiss National Science Foundation professorship at EPFL and in 2005 he was appointed associate professor by EPFL and established the Laboratory of Intelligent Systems. His research interests are Bio-inspired Artificial Intelligence and Robotics. Prof. Floreano is co-founder of the International Society for Artificial Life, Inc., member of the Advisory Group to the European Commission for Future Emerging Technologies, and past-member of the Board of Governors of the International Society for Neural Networks. He published almost 200 peer-reviewed technical papers and edited and co-authored several books, among which *Evolutionary Robotics* with Stefano Nolfi (hardcover 2000; paperback 2004) and *Bioinspired Artificial Intelligence* with Claudio Mattiussi (2008), both by MIT Press. He delivered more than 100 invited talks worldwide, co-organized more than 10 international conferences, and is on the editorial board of 10 international journals.